Accepted Manuscript

Title: A ratiometric electrochemical biosensor for sensitive detection of Hg^{2+} based on thymine-Hg^{2+}-thymine structure

Author: Erhu Xiong Liang Wu Jiawan Zhou Peng Yu Xiaohua Zhang Jinhua Chen

PII: S0003-2670(14)01248-3
DOI: http://dx.doi.org/doi:10.1016/j.aca.2014.10.015
Reference: ACA 233524

To appear in: *Analytica Chimica Acta*

Received date: 24-7-2014
Revised date: 6-10-2014
Accepted date: 11-10-2014

Please cite this article as: Erhu Xiong, Liang Wu, Jiawan Zhou, Peng Yu, Xiaohua Zhang, Jinhua Chen, A ratiometric electrochemical biosensor for sensitive detection of Hg2+ based on thymine-Hg2+-thymine structure, Analytica Chimica Acta http://dx.doi.org/10.1016/j.aca.2014.10.015

A ratiometric electrochemical biosensor for sensitive detection of Hg^{2+} based on thymine-Hg^{2+}-thymine structure

Erhu Xiong, Liang Wu, Jiawan Zhou, Peng Yu, Xiaohua Zhang*, and Jinhua Chen*

State Key Laboratory of Chemo/Biosensing and Chemometrics, College of Chemistry and Chemical Engineering, Hunan University, Changsha, 410082, P. R. China

*Corresponding author. Tel.: +86-731-88821961 E-mail address: chenjinhua@hnu.edu.cn; mickyxie@hnu.edu.cn

Graphical abstract

Highlights

- A ratiometric electrochemical biosensor based on thymine-Hg^{2+}-thymine structure.
- Hg^{2+} was sensitively detected by the developed electrochemical biosensor.
- The ratiometric electrochemical biosensor shows excellent analytical performance.

Abstract

In this paper, a simple, selective and reusable electrochemical biosensor for the sensitive detection of mercury ions (Hg^{2+}) has been developed based on thymine (T)-rich stem-loop (hairpin) DNA probe and a dual-signaling electrochemical ratiometric strategy. The assay strategy includes both "signal-on" and "signal-off" elements. The thiolated methylene blue (MB)-modified T-rich hairpin DNA capture probe (MB-P) firstly self-assembled on the gold electrode surface via Au-S bond. In the presence of Hg^{2+}, the ferrocene (Fc)-labeled T-rich DNA probe (Fc-P) hybridized with MB-P via the Hg^{2+}-mediated coordination of T-Hg^{2+}-T base pairs. As a result, the hairpin MB-P was opened, the MB tags were away from the gold electrode surface and the Fc tags closed to the gold electrode surface. These conformation changes led to the decrease

of the oxidation peak current of MB (I_{MB}), accompanied with the increase of that of Fc (I_{Fc}). The logarithmic value of I_{Fc}/I_{MB} is linear with the logarithm of Hg^{2+} concentration in the range from 0.5 nM to 5000 nM, and the detection limit of 0.08 nM is much lower than 10 nM (the U.S. Environmental Protection Agency (EPA) limit of Hg^{2+} in drinking water). What's more, the developed DNA-based electrochemical biosensor could be regenerated by adding cysteine and Mg^{2+}. This strategy provides a simple and rapid approach for the detection of Hg^{2+}, and has promising application in the detection of Hg^{2+} in real environmental samples.

Keywords: Electrochemistry; Ratiometric biosensor; Methylene blue; Ferrocene; Mercury ion

1. Introduction

As we all know, Hg^{2+} is the most stable modality of inorganic mercury [1]. It is a highly toxic heavy metal ion due to its accumulative character and toxic properties in the environment and biota [2,3]. Long-term exposure to high level of mercury ion can lead to a lot of severe health problems, such as brain damage, kidney failure and other chronic diseases [4]. Therefore, the sensitive, rapid, selective and cost-effective analysis of Hg^{2+} in the environment and food industry is very important. Till now, many kinds of analytical techniques for the detection of Hg^{2+} were reported, such as cold-vapor atomic fluorescence spectroscopy (CV-AFS) [5-7], cold-vapor atomic absorption spectrometry (CV-AAS) [5,8,9], inductively coupled plasma-mass spectrometry (ICP-MS) [10-12], inductively coupled plasma-atomic emission spectrometry (ICP-AES) [13,14]. However, these methods require either expensive instrument or complicated sample preparation processes.

Electrochemical method is a general and classic technique in analytical chemistry because of its advantages of simplicity, high sensitivity, good selectivity and low cost [15-17]. It has been proved that Hg^{2+} ion can selectively bind between two DNA thymine (T) bases and promotes these T-T mismatches to form stable T-Hg^{2+}-T base pairs [18,19], and the binding constant (K_b) of T-Hg^{2+}-T is about 4.14×10^6 L mol^{-1}, higher than that of A (adenine)-T [20,21]. Based on this principle, many DNA-based electrochemical biosensors have been developed for the detection of Hg^{2+}. These electrochemical biosensors could be divided into "signal off" and "signal on" subgroups. In the past years, the DNA-based electrochemical biosensors with "signal off" architecture have gained substantial development. Yu's group [22,23] reported the electrochemical Hg^{2+} biosensors based on the decrease of the electrochemical signal resulting from target-induced conformational changes. However, such "signal-off" sensors suffer from the limited signaling capacity, in which only a maximum of 100% signal suppression can be attained under any experimental conditions [24]. To circumvent this limitation, several "signal on" electrochemical Hg^{2+} biosensors have been reported in recent years. Kim's group [25] and Yang's group [26] developed the "signal on" electrochemical Hg^{2+} biosensors based on the increase of the electrochemical signal resulting from the structural switching of Fc-tagged aptamers immobilized on the electrode surface in the presence of the target analyte. Nevertheless, these electrochemical biosensors were based on the single signal response mechanism. It is no doubt that combination of "signal off" and "signal on" strategies in one DNA-based electrochemical biosensor would have obvious advantages, such as high sensitivity, good selectivity and diversification of data analysis. Up to now, only a few works were reported for the detection of ATP [27], sequence of H5N1 virus [28], protein [29], approximate target mismatch location

[30] based on this strategy. To the best of our knowledge, there are no works to address the Hg^{2+} detection based on the combination of "signal off" and "signal on" strategies.

On the other hand, ratiometric detection has been applied in fluorescence and electrochemiluminescence analysis of biomolecules extensively due to its good characteristics (such as self-calibration, low detection limit) [31-33]. In this work, a simple, selective and reusable electrochemical biosensor for the sensitive detection of mercury ions (Hg^{2+}) has been developed for the first time based on T-rich stem-loop (hairpin) DNA probe and a dual-signaling electrochemical ratiometric strategy (Scheme 1). The thiolated methylene blue (MB)-modified T-rich DNA capture probe (MB-P) self-assembled onto the gold electrode surface via Au-S bond. In the presence of Hg^{2+}, the ferrocene (Fc)-labeled T-rich DNA probe (Fc-P) hybridized with MB-P via the Hg^{2+}-mediated coordination of T-Hg^{2+}-T base pairs. As a result, the hairpin DNA probes (MB-P) were opened, the MB tags were away from the gold electrode surface and the Fc tags close to the gold electrode surface. These conformation changes led to a decrease of the oxidation peak current of MB (I_{MB}) and an increase of that of Fc (I_{Fc}). Based on the logarithmic value of I_{Fc}/I_{MB}, Hg^{2+} was detected sensitively and selectively. What's more, the developed DNA-based electrochemical biosensor could be regenerated by adding cysteine and Mg^{2+} based on the strong binding effect between cysteine and Hg^{2+} [34-36].

2. Experimental section

2.1. Chemicals

The thiolated MB-modified T-rich hairpin DNA capture probe and the Fc-labeled T-rich DNA probe were designed and synthesized by Sangon Biotechnology Co., Ltd (Shanghai, China). The base sequences of MB-P and Fc-P are 5'-SH-$(CH_2)_6$-

GGCGACGTTTTGTCGCC-$(CH_2)_6$-MB-3' and 5'-GACTTTTCGTGCGG-$(CH_2)_6$-Fc-3', respectively. 6-mercaptohexanol (MCH), Tris-(2-carboxyethyl) phosphine hydrochloride (TCEP) and cysteine were purchased from Sigma-Aldrich. Metal salts ($HgCl_2$, $CaCl_2$, $FeCl_3$, $Ni(NO_3)_2$, $Zn(NO_3)_2$, $Pb(NO_3)_2$, $Co(NO_3)_2$, $AlCl_3$, $CdCl_2$, $CrCl_3$, $MgCl_2$, NaCl, KCl, K_2HPO_4, KH_2PO_4, $K_3Fe[CN]_6$, $K_4Fe[CN]_6$) were supplied by Sinopharm Chemical Reagent Co., Ltd (Shanghai, China) and used without further purification. Aqueous solutions used throughout were prepared with ultra pure water (>18 MΩ cm) obtained from a Millipore system.

2.2. Apparatus

All electrochemical measurements, including differential pulse voltammetry (DPV), cyclic voltammetry (CV), electrochemical impedance spectroscopy (EIS), were performed on a CHI660D Electrochemical Workstation (Chenhua Instrument Company of Shanghai, China) at room temperature. A conventional three-electrode cell was used with a planar gold electrode (2 mm in diameter) as the working electrode, a platinum wire as the counter electrode and a saturated calomel electrode (SCE) as the reference electrode. All the potentials were referred to SCE.

2.3. Preparation of the MCH/MB-P/Au electrode

Gold electrode was firstly polished to a mirror-like surface with 0.5 and 0.05 μm alumina slurries, followed by ultrasonication in ultra pure water and methanol. The electrodes were then pretreated by electrochemical oxidation and reduction in 0.5 M H_2SO_4 aqueous solution by potential cycling in the potential between -0.3 and 1.5 V with a scan rate of 100 mV s^{-1} until the cyclic voltammogram characteristic for a clean gold electrode was obtained. Then, the gold electrode was washed with copious amounts of ultra pure water and dried under nitrogen gas.

Before immobilization onto the gold electrode surface, the MB-P was dissolved in 100 mM Tris-HCl buffer solution (containing 0.5 M NaCl, 5 mM $MgCl_2$, 10 mM TCEP, PH 7.4) and incubated in the dark for 1 h to reduce disulfide bunds. Then, 10 μL of 1 μM MB-P solution was placed onto the cleaned gold electrode surface for 16 h at room temperature to obtain the MB-P/Au electrode. The MB-P/Au electrode was further immersed into 2 mM MCH solution with 10 mM Tris-HCl buffer solution for 1 h to block the uncovered gold electrode surface as well as to make the array of ss-DNA on the electrode interface more regular. The obtained electrode was labeled as the MCH/MB-P/Au electrode. To monitor each immobilization step, the electrochemical impedance measurements were performed in 0.1 M KCl aqueous solution with 5 mM $[Fe(CN)_6]^{3-/4-}$ as the probe in the frequency range from 0.1 Hz to 100 kHz with 5 mV as the amplitude at a potential of 0.22 V (vs. SCE).

2.4. Electrochemical detection of Hg^{2+}

The MCH/MB-P/Au electrode was incubated in 10 mM phosphate buffer solution (PBS) containing 0.5 M NaCl (pH 7.4) with 1 μM Fc-P and different concentrations of Hg^{2+} at room temperature for 2 h, leading to the opening of hairpin (stem-loop) structure of MB-P and the formation of the double helix DNA structure through the specific T-Hg^{2+}-T complexes. Then the electrochemical performance of the electrode was investigated by DPV in 4 mL of 10 mM PBS (pH 7.4) containing 0.5 M NaCl, 5 mM $MgCl_2$. Each measurement was repeated at least three times, and the control experiments for various metal ions were performed under the same conditions. After the detection of Hg^{2+}, the biosensor was regenerated by immersing the electrode into 4 mL of 10 mM PBS (pH 7.4) containing 0.5 M NaCl, 5 mM $MgCl_2$ and 10 μM cysteine for 2 h. After washed with 10 mM PBS (pH 7.4), the regenerated electrode could be reused for another assay.

3. Results and discussion

3.1. Characterization of the electrochemical Hg^{2+} biosensor

As one of the electrochemical technologies, EIS has been proven as one of the most powerful tools for interfacial investigation [37]. In a typical electrochemical impedance spectrum, the semicircle portion observed at higher frequencies corresponds to the charge-transfer limited process and the increase of the diameter of the semicircle reflects the increase of the interfacial charge-transfer resistance (Rct) [38]. As shown in Fig. 1A, the bare gold electrode shows a very small semicircle domain (Rct = 100 Ω, curve a), indicating a very fast charge-transfer process. After the immobilization of MB-P on the gold electrode surface, the Rct of the electrode increases to 2700 Ω (curve b) due to the effective repulsion between the negatively charged MB-P and $[Fe(CN)_6]^{3/4}$ anions. Subsequent surface blocking with 6-mercaptohexanol (MCH) also leads to an obvious increase in Rct (Rct = 4300 Ω, curve c). After hybridizing with Fc-P based on the T-Hg^{2+}-T structure, the Rct increases significantly (Rct = 8200 Ω, curve d). For the regeneration of the developed electrochemical biosensor, the above electrode was immersed into 10 mM PBS containing 10 μM cysteine and 5 mM Mg^{2+}. It is noted that the Rct decreases to 4400 Ω (curve e) due to the dissociation of Fc-P from the double helix structure.

The electrochemical biosensor was also characterized by CV. As shown in Fig. 1B, compared with the bare gold electrode (curve a), the peak current of the MB-P modified electrode (curve b) decreases obviously and the peak-to-peak separation increases, which indicates that the MB-P strand is immobilized successfully on the gold electrode surface. After the surface of the MB-P/Au electrode is blocked by MCH, the peak current decreases correspondingly (curve c). In the presence of Hg^{2+}, the peak current further decreases (curve d) due to the hybridization between MB-P

and Fc-P based on the T-Hg^{2+}-T structure. However, when the above electrode was immersed into 10 mM PBS containing 10 μM cysteine and 5 mM Mg^{2+}, the peak current increases and the peak-to-peak separation decreases markedly (curve e). These results are in accordance with that observed in EIS investigation (Fig. 1A) and demonstrate that the electrochemical biosensor has been fabricated successfully according to Scheme 1.

3.2. Feasibility of the electrochemical Hg^{2+} biosensor

To demonstrate the feasibility of the developed electrochemical biosensor, DPV responses of the different modified electrodes were investigated. As shown in Fig. 2, the MCH/MB-P/Au electrode has only one large oxidation peak of MB at about -0.28 V (curve a). When the MCH/MB-P/Au electrode was further incubated with Fc-P and without Hg^{2+}, no obvious change of the oxidation peak current of MB is observed (curve b), indicating that the hybridization between MB-P and Fc-P does not happen in the absence of Hg^{2+}. However, after incubating the MCH/MB-P/Au electrode in the solution with both Fc-P and Hg^{2+}, the oxidation peak current of MB decreases obviously and another oxidation peak which should correspond to the oxidation of Fc can be observed at about 0.29 V (curve c). These should result from the opening of the hairpin structure of MB-P and the successful construction of the double helix DNA structure between Fc-P and MB-P according to Scheme 1 by the formation of T-Hg^{2+}-T. The above conformation changes result in that the MB tags are away from the gold electrode surface and the Fc tags close to the gold electrode surface. After the electrode was further incubated in 10 mM PBS containing 1 μM cysteine and 5 mM Mg^{2+}, cysteine could bind Hg^{2+} more effectively and Mg^{2+} could induce the formation of the hairpin structure of MB-P via tailor-made complementary bases at both ends [39,40], resulting in the dissociation of Fc-P from the double helix structures. As the

result, the oxidation peak current of MB increases and that of Fc decreases (curve d). These results indicate clearly that the developed electrochemical biosensor can be used to detect Hg^{2+} and regenerated effectively.

3.3. Electrochemical assay of Hg^{2+}

Keeping the concentration of Fc-P at 1 μM, the DPV responses of the MCH/MB-P/Au electrode to the different concentrations of Hg^{2+} were shown in Fig. 3. From Fig. 3A, it is noted that the oxidation peak current of MB decreases and the oxidation peak current of Fc increases with the increase of Hg^{2+} concentration. Based on the individual MB or Fc signal for Hg^{2+} detection, the dependence of the oxidation peak current of MB (or Fc) on the concentration of Hg^{2+} is shown in Fig. 3B. In the range of 0.5 nM to 1000 nM, both of them exhibit good linear relationship between the oxidation peak current and the logarithm of Hg^{2+} concentration, and the detection limits are 0.34 nM (based on MB signal) and 0.28 nM (based on Fc signal) (S/N = 3), respectively. The insert plot in Fig. 3A shows the calibration plot of the electrochemical ratiometric assay of Hg^{2+} using I_{Fc}/I_{MB} as signal. The logarithmic value of I_{Fc}/I_{MB} is also linear with the logarithm of Hg^{2+} concentration in the range from 0.5 nM to 5000 nM with the detection limit of 0.08 nM (S/N = 3), and the linear regression equation is:

$$\lg(I_{Fc}/I_{MB}) = 0.5768\lg C - 0.7497 \ (R^2 = 0.9969) \quad (1)$$

It is noted that the obtained detection limit (0.08 nM) is 125 times lower than the limit of Hg^{2+} in drinking water (10 nM) by U.S. Environmental Protection Agency (EPA) [41-43]. On the other hand, it is worthy to note that the electrochemical ratiometry exhibits a wider linear range and lower detection limit than the typical electrochemical methods based on single signal response mechanism. The detection

limit of the proposed method is also lower than that of many electrochemical Hg^{2+} biosensors reported previously (Table 1).

3.4. Regeneration, stability and selectivity of the electrochemical biosensor

The regeneration of the electrochemical biosensor is very important in its practical application. As shown in Fig. 4, the biosensor can be readily regenerated after the Hg^{2+} assay by immersing the electrode into 10 mM PBS containing 10 μM cysteine and 5 mM Mg^{2+} for 2 h. It is noted from Fig. 4 that after five cycles of regeneration process, both MB and Fc signals are almost recovered to the original values, indicating the developed electrochemical biosensor can be easily regenerated and reused.

The reproducibility of the MCH/MB-P/Au electrode was also evaluated. Five modified electrodes were used to detect Hg^{2+} and the relative standard deviation is 3.7%. Furthermore, the MCH/MB-P/Au electrode was stored in the refrigerator at 4 ^{o}C for two weeks and no obvious change of the response current was observed. These indicate that the developed electrochemical biosensor has satisfactory reproducibility and stability.

To investigate the selectivity of the developed electrochemical Hg^{2+} biosensor, various metal ions that exist in real samples commonly, such as Al^{3+}, Ba^{2+}, Cd^{2+}, Co^{2+}, Cr^{3+}, Fe^{3+}, Mn^{2+}, Pb^{2+} and Zn^{2+}, replaced Hg^{2+} in the hybridization buffer and the corresponding results are shown in Fig. 5. As shown in Fig. 5, the I_{Fc}/I_{MB} value of the sensor in the presence of Hg^{2+} is at least 280 times larger than that in the presence of other metal ions. This indicates clearly that the developed electrochemical biosensor possesses excellent selectivity for Hg^{2+} detection.

4. Recovery test

In order to evaluate the applicability and reliability of the developed electrochemical biosensor, the recovery experiments for different Hg^{2+} concentrations were carried out in real water samples that were collected from local river (Xiangjiang River) and local tap water. Prior to use, the local river water should be centrifugated to remove the impurities (such as sands). These water samples were diluted 10 times with 100 mM PBS, and then spiked with different concentrations of Hg^{2+}. From Table 2, it is noted that the recoveries for the added Hg^{2+} with 2.0 nM, 5.0 nM, 10.0 nM, 50.0 nM are 103.0%, 98.4%, 97.1% and 98.5%, respectively. These results indicated that the recovery of the developed electrochemical Hg^{2+} biosensor is satisfactory and the proposed method may have great promising applications in monitoring of the mercury ion in real environmental samples.

On the other hand, the analytical performance of the proposed method was further evaluated by the detection of Hg^{2+} in human serum samples which were obtained from healthy individuals. Hg^{2+} with different concentrations was added in 10-fold diluted human serum sample solutions which diluted with 100 mM PBS. The biological exposure index for Hg^{2+} defined by American Conference of Governmental Industrial Hygienists (ACGIH) in blood samples is 1.5 μg/100 mL (75 nM) [49]. Thus, the concentrations of Hg^{2+} in human serum were chosen to be 10 nM, 30 nM and 50 nM, which were below the stated level. As shown in Table 3, the recoveries for the added Hg^{2+} are 102.6%, 96.4% and 100.9%, respectively. These results indicate that the developed electrochemical biosensor has potential application for Hg^{2+} detection in complex biological samples.

5. Conclusions

Based on the T-rich stem-loop (hairpin) DNA probe and a dual-signaling electrochemical ratiometric strategy, a new electrochemical Hg^{2+} biosensor has been developed. Compared with the typical single-signaling electrochemical sensor, the developed electrochemical biosensor has a wider linear response range (0.5 nM to 5000 nM) and lower detection limit (0.08 nM, S/N = 3) for Hg^{2+} detection. What's more, the developed DNA-based electrochemical biosensor has excellent selectivity and reproducibility, and could be easily regenerated by adding cysteine and Mg^{2+}. We believe that our new analytical method will have great promising applications in monitoring of the mercury ion in real environmental samples.

Acknowledgements

This work was financially supported by NSFC (21275041, 21235002), the Foundation for Innovative Research Groups of NSFC (21221003), Hunan Provincial Natural Science Foundation of China (12JJ2010), the Specialized Research Fund for the Doctoral Program of Higher Education (20110161110009), and PCSIRT (IRT1238).

References

[1] L. Qi, Y.X. Zhao, H. Yuan, K. Bai, Y. Zhao, F. Chen, Y.H. Dong, Y.Y. Wu, Amplified fluorescence detection of mercury (II) ions (Hg^{2+}) using target-induced DNAzyme cascade with catalytic and molecular beacons, Analyst 137 (2012) 2799-2805.

[2] P.B. Tchounwou, W.K. Ayensu, N. Ninashvili, D. Suttton, Environmental exposure to mercury and its toxicopathologic implications for public health, Environ. Toxicol. 18 (2003) 149-175.

[3] Q.R. Wang, D. Kim, D.D. Dionysiou, G.A. Sorial, D. Timberlake, Sources and remediation for mercury contamination in aquatic systemsda literature review, Environ. Pollut. 131 (2004) 323-336.

[4] L. Zhang, H.X. Chang, A. Hirata, H.K. Wu, Q.K. Xue, M.W. Chen, Nanoporous gold based optical sensor for sub-ppt detection of mercury ions, ACS Nano 7 (2013) 4595-4600.

[5] H. Erxleben, J. Ruzicka, Atomic absorption spectroscopy for mercury, automated by sequential injection and miniaturized in lab-on-valve system, Anal. Chem. 77 (2005) 5124-5128.

[6] Y.K. Li, Y.R. Xu, Y. Huang, Y. Dai, Q.F. Hu, G.Y. Yang, Cold vapour generation and atomic fluorescence spectrometry for the determination of mercury, Chem. Asian J. 21 (2009) 2893-2897.

[7] M. Leermakers, W. Baeyens, P. Quevauviller, M. Horvat, Mercury in environmental samples: speciation, artifacts and validation, TrAC, Trends Anal. Chem. 24 (2005) 383-393.

[8] N. Ferrua, S. Cerutti, J.A. Salonia, R.A. Olsina, L.D. Martinez, On-line preconcentration and determination of mercury in biological and environmental samples by cold vapor-atomic absorption spectrometry, J. Hazard. Mater. 141 (2007) 693-699.

[9] N. Pourreza, K. Ghanemi, Solid phase extraction of cadmium on 2-mercaptobenzothiazole loaded on sulfur powder in the medium of ionic liquid 1-butyl-3-methylimidazolium hexafluorophosphate and cold vapor generation–

atomic absorption spectrometric determination, J. Hazard. Mater. 178 (2010) 566-571.

[10] J.L. Barriada, A.D. Tappin, E.H. Evans, E.P. Achterberg, Dissolved silver measurements in seawate, TrAC, Trends Anal. Chem. 26 (2007) 809-817.

[11] N.H. Bings, A. Bogaerts, J.A.C. Broekaert, Atomic spectroscopy, Anal. Chem. 78 (2006) 3917-3946.

[12] D. Malinovsky, R.E. Sturgeon, L. Yang, Anion-exchange chromatographic separation of Hg for isotope ratio measurements by multicollector ICPMS, Anal. Chem. 80 (2008) 2548-2555.

[13] B.W. Acon, J.A. Mclean, A. Montaser, A large bore-direct injection high efficiency nebulizer for inductively coupled plasma spectrometry, Anal. Chem. 72 (2000) 1885-1893.

[14] F.X. Han, W.D. Patterson, Y.J. Xia, B.B.M. Sridhar, Y. Su, Rapid determination of mercury in plant and soil samples using inductively coupled plasma atomic emission spectroscopy, a comparative study, Water Air Soil Pollut. 170 (2006) 161-171.

[15] N.J. Ronkainen, H.B. Halsall, W.R. Heineman, Electrochemical biosensors, Chem. Soc. Rev. 39 (2010) 1747-1763.

[16] F. Ricci, K.W. Plaxco, E-DNA sensors for convenient, label-free electrochemical detection of hybridization, Microchim. Acta 163 (2008) 149-155.

[17] E. Bakker, Y. Qin, Electrochemical sensors, Anal. Chem. 78 (2006) 3965-3984.

[18] A. Ono, H. Togashi, Highly selective oligonucleotide-based sensor for mercury (II) in aqueous solutions, Angew. Chem. Int. Ed. 43 (2004) 4300-4302.

[19] Y. Wang, F. Geng, Q. Cheng, H. Xu, M. Xu, Oligonucleotide-based label-free Hg^{2+} assay with a monomer-excimer fluorescence switch, Analyst 136 (2011) 4284-4288.

[20] Y. Li, Y. Jiang, X.P. Yan, Probing mercury species-DNA interactions by capillary electrophoresis with on-line electrothermal atomic absorption spectrometric detection, Anal. Chem. 78 (2006) 6115-6120.

[21] Z.Q. Zhu, Y.Y. Su, J. Li, D. Li, J. Zhang, S.P. Song, Y. Zhao, G.X. Li, C.H. Fan, Highly sensitive electrochemical sensor for mercury (II) ions by using a mercury-specific oligonucleotide probe and gold nanoparticle-based amplification, Anal. Chem. 81 (2009) 7660-7666.

[22] S.J. Liu, H.G. Nie, J.H. Jiang, G.L. Shen, R.Q. Yu, Electrochemical sensor for mercury (II) based on conformational switch mediated by interstrand cooperative coordination, Anal. Chem. 81 (2009) 5724-5730.

[23] D.H. Wu, Q. Zhang, X. Chu, H.B. Wang, G.L. Shen, R.Q. Yu, Ultrasensitive electrochemical sensor for mercury (II) based on target-induced structure-switching DNA, Biosens. Bioelectron. 25 (2010) 1025-1031.

[24] Z.G. Yu, R.Y. Lai, A reagentless and reusable electrochemical DNA sensor based on target hybridization-induced stem-loop probe formation, Chem. Commun. 48 (2012) 10523-10525.

[25] D.H. Han, Y.-R. Kim, J.-W. Oh, T.H. Kim, R.K. Mahajan, J.S. Kim, H. Kim, A regenerative electrochemical sensor based on oligonucleotide for the selective determination of mercury (II), Analyst 134 (2009) 1857-1862.

[26] J.Y. Zhuang, L.B. Fu, D.P. Tang, M.D. Xu, G.N. Chen, H.H. Yang, Target-induced structure-switching DNA hairpins for sensitive electrochemical monitoring of mercury (II), Biosens. Bioelectron. 39 (2013) 315-319.

[27] L. Wu, X.H. Zhang, W. Liu, E.H. Xiong, J.H. Chen, Sensitive electrochemical aptasensor by coupling “signal-on’’ and “signal-off’’ strategies, Anal. Chem. 85 (2013) 8397-8402.

[28] I. Grabowska, K. Malecka, A. Stachyra, A. Góra-Sochacka, A. Sirko, W. Zagórski-Ostoja, H. Radecka, J. Radecki, Single electrode genosensor for simultaneous determination of sequences encoding hemagglutinin and neuraminidase of avian influenza virus type H5N1, Anal. Chem. 85 (2013) 10167-10173.

[29] K.W. Ren, J. Wu, F. Yan, H.X. Ju, Ratiometric electrochemical proximity assay for sensitive one-step protein detection, Sci. Rep. 4 (2014) 4360.

[30] W.W. Yang, R.Y. Lai, Integration of two different sensing modes in an electrochemical DNA sensor for approximation of target mismatch location, Electrochem. Commun. 13 (2011) 989-992.

[31] P. Zhang, T. Beck, W.H. Tan, Design of a molecular beacon DNA probe with two fluorophores, Angew. Chem. Int. Ed. 113 (2001) 416-419.

[32] H.R. Zhang, J.J. Xu, H.Y. Electrochemiluminescence ratiometry: a new approach to DNA biosensing, Chen, Anal. Chem. 85 (2013) 5321-5325.

[33] Y.J. Gong, X.B. Zhang, C.C. Zhang, A.L. Luo, T. Fu, W.H. Tan, G.L. Shen, R.Q. Yu, Through bond energy transfer: a convenient and universal strategy toward efficient ratiometric fluorescent probe for bioimaging applications, Anal. Chem. 84 (2012) 10777-10784.

[34] J.-S. Lee, P.A. Ulmann, M.S. Han, C.A. Mirkin, A DNA-gold nanoparticle-based colorimetric competition assay for the detection of cysteine, Nano lett. 8 (2008) 529-533.

[35] Y. Tian, Z. Zhang, L.P. Wen, J. Ma, Y.Q. Zhang, W.D. Liu, J. Zhai, L. Jiang, A biomimetic mercury (II)-gated single nanochannel, Chem. Commun. 49 (2013) 10679-10681.

[36] H. Xu, M. Hepel, "Molecular Beacon"-based fluorescent assay for selective detection of glutathione and cysteine, Anal. Chem. 83 (2011) 813-819.

[37] A. Bardea, F. Patolsky, A. Dagan, I. Willner, Sensing and amplification of oligonucleotide-DNA interactions by means of impedance spectroscopy: a route to a tay-sachs sensor, Chem. Commun. (1999) 21-22.

[38] Y. Cao, S. Zhu, J.C. Yu, X.J. Zhu, Y.M. Yin, G.X. Li, Protein detection based on small molecule-linked DNA, Anal. Chem. 84 (2012) 4314-4320.

[39] V.V. Dao, R.H. Guenther, P.F. Agris, The role of 5-methylcytidine in the anticodon arm of yeast tRNAPhe: site-specific magnesium binding and coupled conformational transition in DNA analogs, Biochem. 31 (1992) 11012-11019.

[40] N.B. Ramsing, K. Rippe, T.M. Jovin, Helix-coil transition of parallel-stranded DNA. Thermodynamics of hairpin and linear duplex oligonucleotides, Biochem. 28 (1989) 9528-9535.

[41] E.M. Nolan, S.J. Lippard, Tools and tactics for the optical detection of mercuric ion, Chem. Rev. 108 (2008) 3443-3480.

[42] F. Xuan, X.T. Luo, I.-M. Hsing, Conformation-dependent exonuclease III activity mediated by metal ions reshuffling on thymine-rich DNA duplexes for an ultrasensitive electrochemical method for Hg^{2+} detection, Anal. Chem. 85 (2013) 4586-4593.

[43] Office of Water. Mercury Update: Impact on Fish Advisories, EPA Fact Sheet EPA-823-F-01-011; U.S. Environmental Protection Agency: Washington, DC, 2001.

[44] Z.P. Zhang, A. Tang, S.Z. Liao, P.F. Chen, Z.Y. Wu, G.L. Shen, R.Q. Yu, Oligonucleotide probes applied for sensitive enzyme-amplified electrochemical assay of mercury (II) ions, Biosens. Bioelectron. 26 (2011) 3320-3324.

[45] X.H. Niu, Y.L. Ding, C. Chen, H.L. Zhao, M.B. Lan, A novel electrochemical biosensor for Hg^{2+} determination based on Hg^{2+}-induced DNA hybridization, Sens. Actuat. B 158 (2010) 383-387.

[46] R.G. Cao, B. Zhu, J.J. Li, D.S. Xu, Oligonucleotides-based biosensors with high sensitivity and selectivity for mercury using electrochemical impedance spectroscopy, Electrochem. Commun. 11 (2009) 1815-1818.

[47] R.M. Kong, X.B. Zhang, L.L. Zhang, X.Y. Jin, S.Y. Huan, G.L. Shen, R.Q. Yu, An ultrasensitive electrochemical ‘‘turn-on’’ label-free biosensor for Hg^{2+} with AuNP-functionalized reporter DNA as a signal amplifier, Chem. Commun. (2009) 5633-5635.

[48] Y.Q. Lai, Y.Y. Ma, L.P. Sun, J. Jia, J. Weng, N. Hu, W. Yang, Q.Q. Zhang, A highly selective electrochemical biosensor for Hg^{2+} using hemin as a redox indicator, Electrochim. Acta 56 (2011) 3153-3158.

[49] American Conference of Governmental Industrial Hygienists. TLVs and BEIs. Threshold Limit Values for Chemical Substances and Physical Agents and Biological Exposure Indices. ISBN: 1-882417-49-6, Cincinnati, OH, 2003.

Figure Captions

Scheme 1. Schematic illustration of the ratiometric electrochemical biosensor for Hg^{2+} detection.

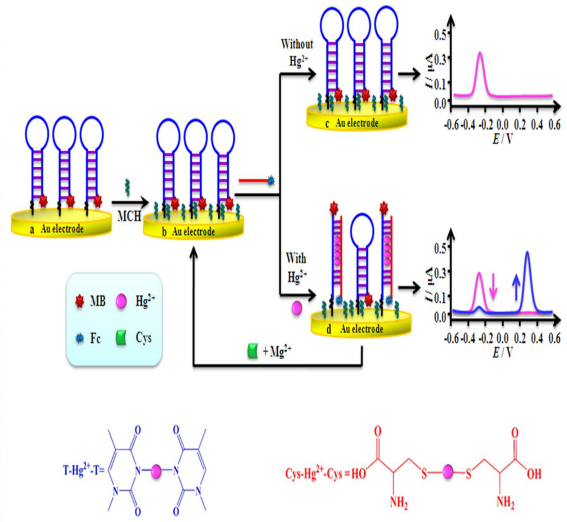

Fig. 1. (A) Electrochemical impedance spectra (Nyquist plots) of the different modified electrodes in 0.1 M KCl aqueous solution containing 5 mM (1:1) $[Fe(CN)_6]^{3-/4-}$ in the frequency range from 0.1 Hz to 100 kHz with 5 mV as the amplitude at a potential of 0.22 V and (B) Cyclic voltammograms obtained in 0.1 M KCl aqueous solution containing 5 mM (1:1) $[Fe(CN)_6]^{3-/4-}$ at a scan rate of 100 mV s^{-1}. (a) bare Au electrode, (b) MB-P/Au electrode, (c) MCH/MB-P/Au electrode, (d) MCH/MB-P/Au electrode after incubated with Fc-P and Hg^{2+}, (e) electrode of (d) after regenerated in 10 mM PBS containing 10 μM cysteine and 5 mM Mg^{2+}.

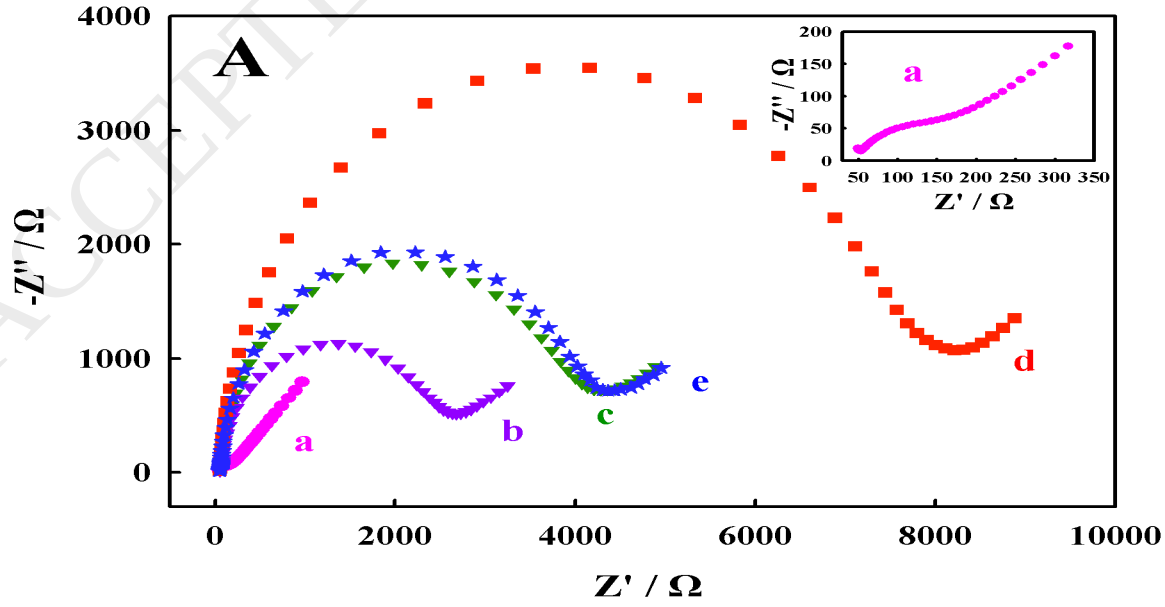

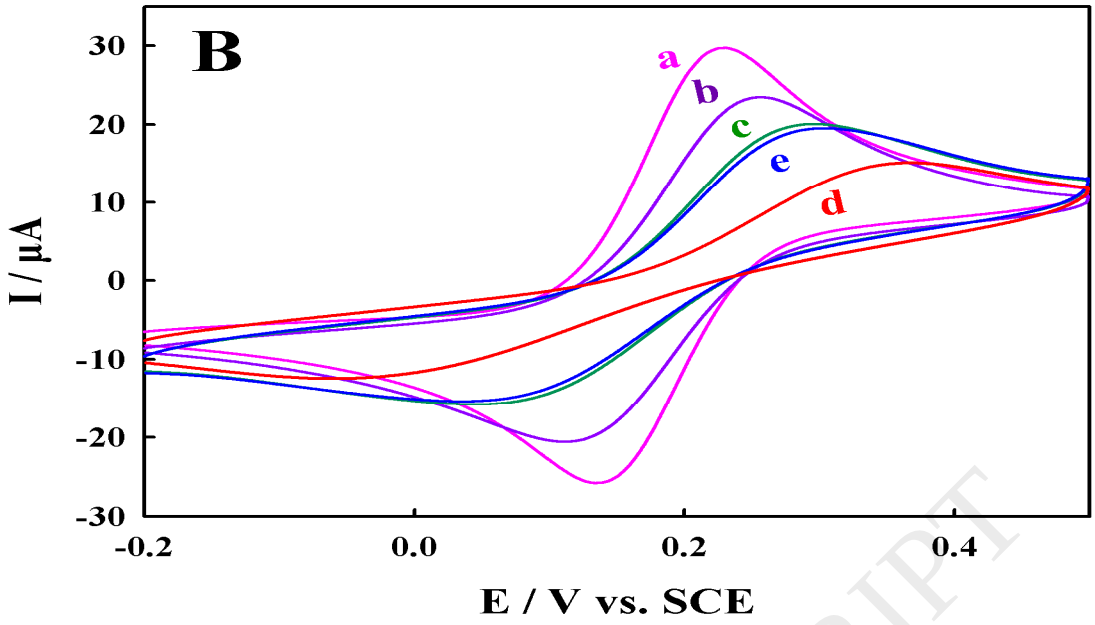

Fig. 2. DPV curves of the different electrodes. (a) MCH/MB-P/Au electrode, (b) MCH/MB-P/Au electrode with Fc-P in the absence of Hg^{2+}, (c) MCH/MB-P/Au electrode with Fc-P in the presence of Hg^{2+}, and (d) electrode of (c) further incubated with 10 mM PBS containing 1 μM cysteine and 5 mM Mg^{2+}.

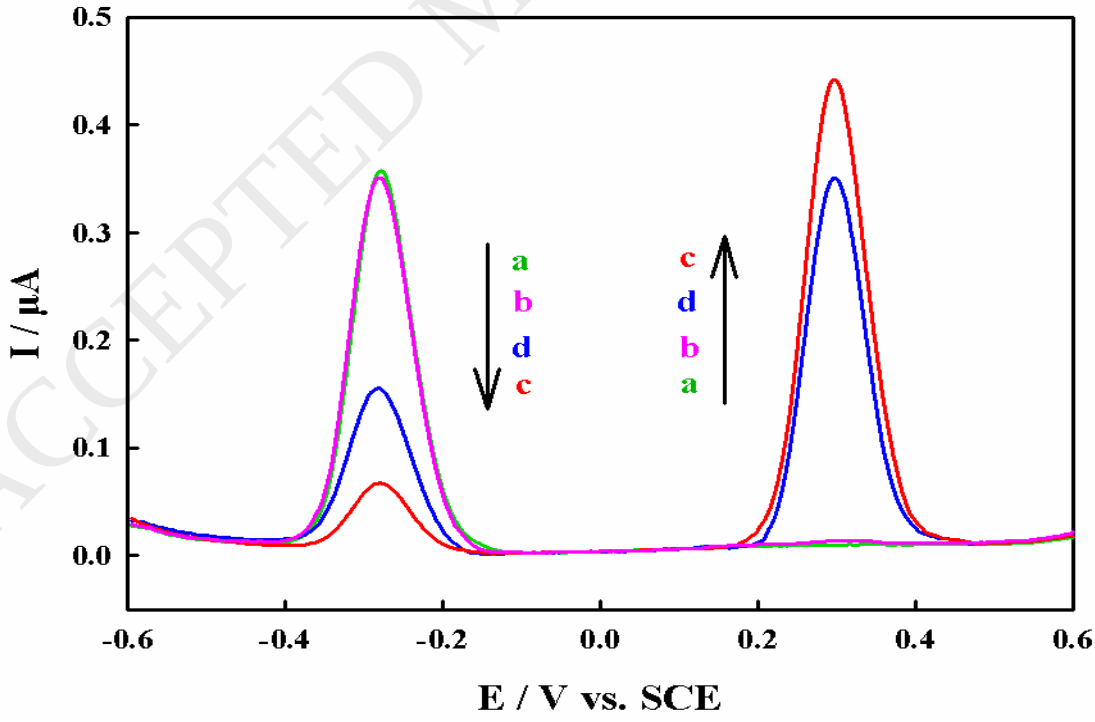

Fig. 3. (A) DPV curves for the detection of different concentrations of Hg^{2+}. The concentrations are (from a to k) 0 nM, 0.5 nM, 1 nM, 5 nM, 10 nM, 50 nM, 100 nM, 200 nM, 500 nM, 1 μM and 5 μM. Inset: logarithmic dependence of I_{Fc}/I_{MB} on Hg^{2+} concentration. (B) The linear fit plots of the MB and Fc peak currents as function of the logarithm of Hg^{2+} concentration. Error bar represents the standard deviation of three parallel experiments.

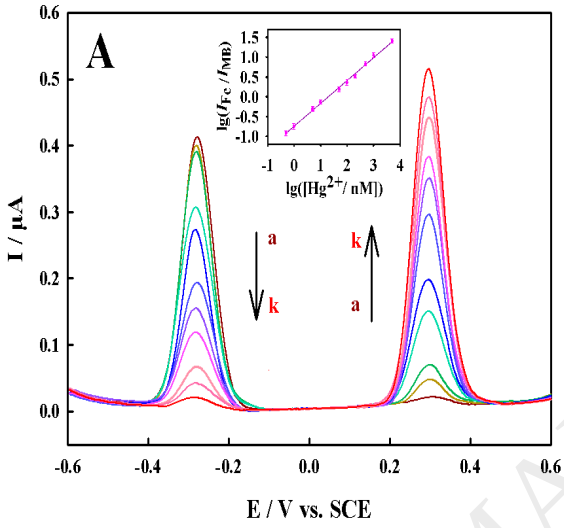

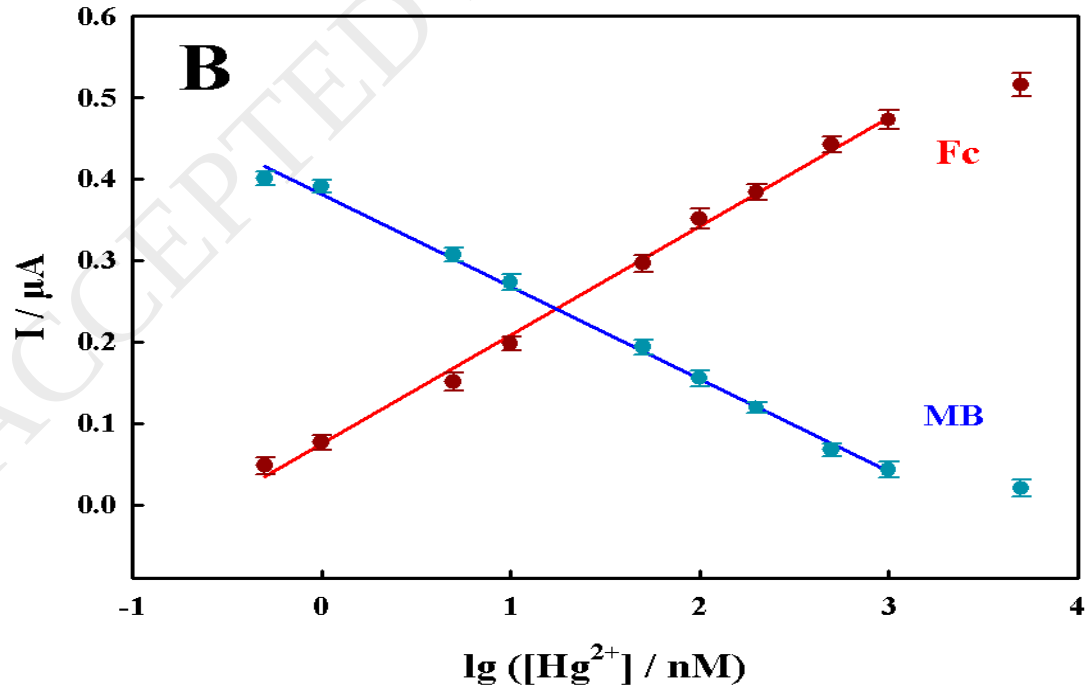

Fig. 4. Regeneration of the electrochemical Hg^{2+} biosensor with the stepwise interaction with Hg^{2+} and then cysteine. N represents the regeneration times of the sensor.

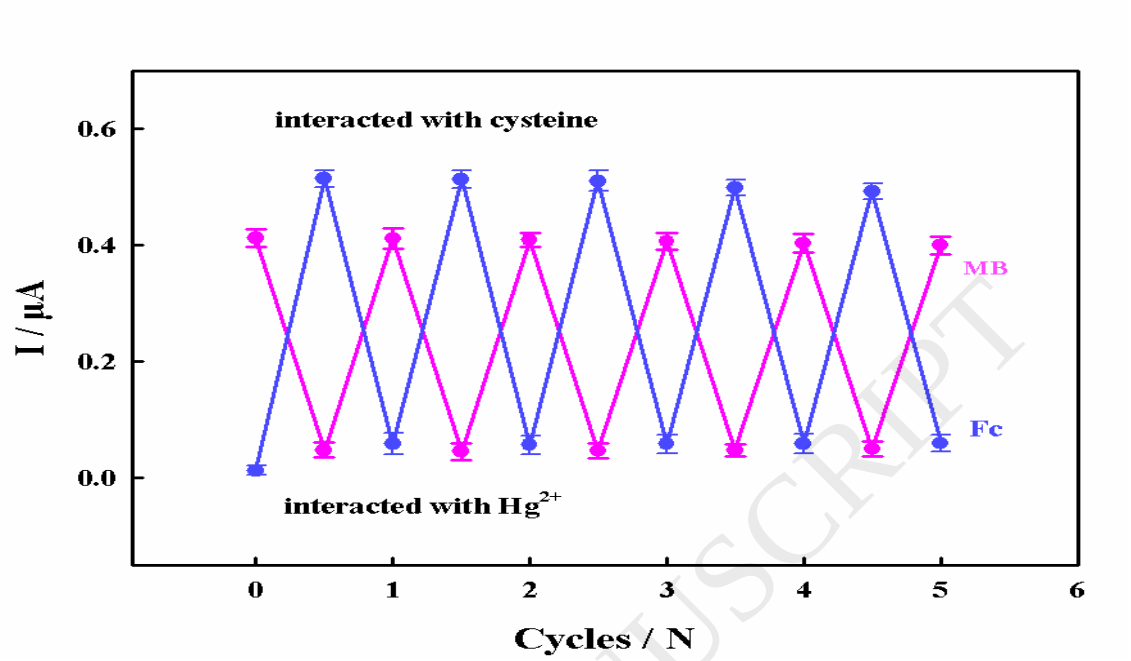

Fig. 5. Selectivity of the electrochemical Hg^{2+} biosensor. Concentration of Hg^{2+} is 5 μM and the others are 10 μM. Error bar represents the standard deviation of three parallel experiments.

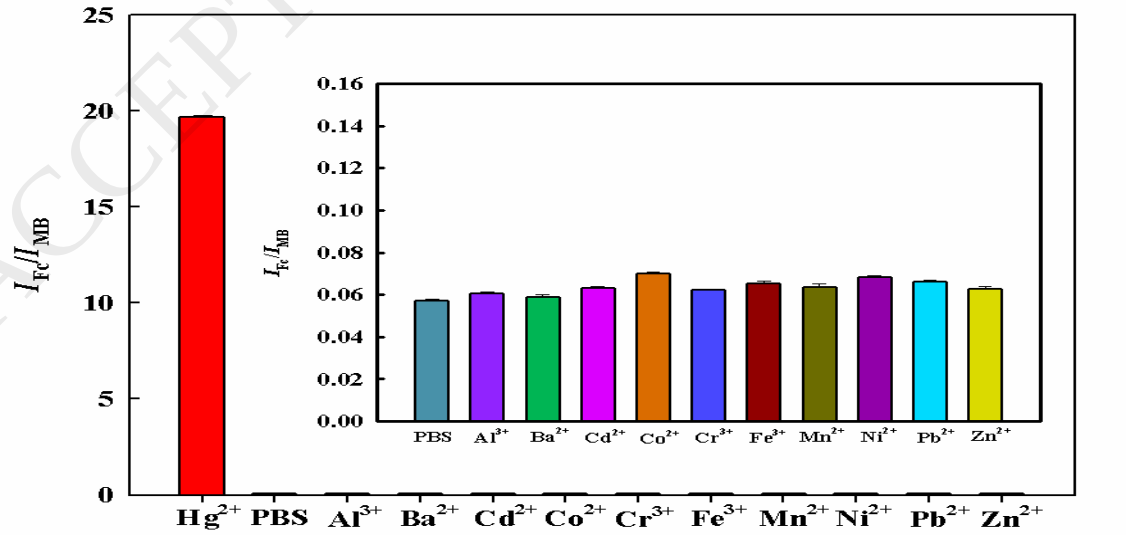

Table 1. Comparison of some electrochemical biosensors for Hg^{2+} detection[a]

Method	Probe	Detection limit	Linear range	Reference
CV	HRP	0.3 nM	0.5 nM~1 μM	[44]
CV	Fc	0.6 nM	1 nM~10 μM	[45]
EIS	label-free	0.1 nM	1 nM~1 mM	[46]
SWV	Fc	2.5 nM	5 nM~1 μM	[26]
SWV	Au NPs	0.5 nM	0.5 nM~100 nM	[21]
DPV	MB	0.5 nM	1 nM~0.1 μM	[47]
DPV	Fc	0.5 nM	1 nM~2 μM	[22]
DPV	Fc	100 nM	0.1 μM~2 μM	[25]
DPV	Hemin	50 nM	0~2 μM	[48]
DPV	MB and Fc	0.08 nM	0.5 nM~5 μM	present work

[a]Abbreviation: cyclic voltammetry (CV), electrochemical impedance spectroscopy (EIS), square wave voltammetry (SWV), differential pulse voltammetry (DPV), horse radish peroxidase (HRP), ferrocene (Fc), methylene blue (MB)

Table 2. Recovery assays of Hg^{2+} in real environmental samples with the proposed method.

Sample	Added [Hg^{2+}] / nM	Found (nM)	Recovery (%)
Tap Water 1	2.0	2.06±0.15	103.0
Tap Water 2	5.0	4.92±0.28	98.4
River Water 1	10.0	9.71±0.33	97.1
River Water 2	50.0	49.27±0.59	98.5

Table 3. Recovery assays of Hg^{2+} in 10-fold diluted human serum samples.

Sample (No.)	Added [Hg^{2+}] / nM	Found (nM)	Recovery (%)
1	10	10.26±0.13	102.6
2	30	28.93±0.34	96.4
3	50	50.47±0.22	100.9